Published in final edited form as:
*J Cell Physiol*. 2012 January ; 227(1): 278–287. doi:10.1002/jcp.22733.

# Chromosomal instability in mouse embryonic fibroblasts null for the transcriptional co-repressor Ski

**Katherine Marcelain**[1,3,*], **Ricardo Armisen**[2,3], **Adam Aguirre**[3], **Nobuhide Ueki**[4], **Jessica Toro**[1], **Clemencia Colmenares**[5], and **Michael J Hayman**[4]

[1] Programa de Genética Humana, Instituto de Ciencias Biomédicas, Facultad de Medicina, Universidad de Chile. Santiago, Chile

[2] Programa de Fisiopatología, Instituto de Ciencias Biomédicas, Facultad de Medicina, Universidad de Chile. Santiago, Chile

[3] Centro de Estudios Moleculares de la Célula, Facultad de Medicina, Universidad de Chile, Santiago, Chile

[4] Microbiology and Molecular Genetics Department, Stony Brook University, Stony Brook, New York, USA

[5] Department of Cancer Biology, Lerner Research Institute, Cleveland Clinic Foundation, Cleveland. Ohio, USA

## Abstract

Ski is a transcriptional regulator that has been considered an oncoprotein, given its ability to induce oncogenic transformation in avian model systems. However, studies in mouse and in some human tumor cells have also indicated a tumor suppressor activity for this protein. We found that *Ski*−/− mouse embryo fibroblasts exhibit high levels of genome instability, namely aneuploidy, consistent with a tumor suppressor function for Ski. Time-lapse microscopy revealed lagging chromosomes and chromatin/chromosome bridges as the major cause of micronuclei formation and the subsequent aneuploidy. Although these cells arrested in mitosis after treatment with spindle disrupting drugs and exhibited a delayed metaphase/anaphase transition, Spindle Assembly Checkpoint (SAC) was not sufficient to prevent chromosome missegregation, consistent with a weakened SAC. Our *in vivo* analysis also showed dynamic metaphase plate rearrangements with switches in polarity in cells arrested in metaphase. Importantly, after ectopic expression of Ski the cells that displayed this metaphase arrest died directly during metaphase or after aberrant cell division, relating SAC activation and mitotic cell death. This increased susceptibility to undergo mitosis-associated cell death reduced the number of micronuclei-containing cells. The presented data support a new role for Ski in the mitotic process and in maintenance of genetic stability, providing insights into the mechanism of tumor suppression mediated by this protein.

### Keywords

Ski; Aneuploidy; time-lapse; chromosome segregation; weakened SAC; mitotic catastrophe

[*]Corresponding Author. Mailing Address: Independencia 1027. Independencia. Santiago 7-Chile. Phone: (562)9786741. Fax: (562)7373158. kmarcelain@med.uchile.cl.

## Introduction

Ski was first identified in a series of avian retroviruses isolated at the Sloan Kettering Institute (Li et al., 1986; Stavnezer et al., 1986). Although it has been described that Ski acts as a transcriptional co-activator of certain genes (Chen et al., 2003; Zhang and Stavnezer, 2009), the more established function for this protein is to act as anegative regulator in several signal transductionpathways, including TGF-β (Akiyoshi et al., 1999; Luo et al., 1999; Sun et al., 1999; Xu et al., 2000) and nuclear hormone receptorsignaling (Dahl et al., 1998). In these and other pathways, Ski acts as a transcriptional repressor primarilydue to multiple direct and indirect interactions with histonedeacetylase (HDAC) (Nomura et al., 1999; Tabata et al., 2009; Ueki et al., 2008; Zhao et al., 2009) complexes including N-CoR/SMRT/Sin3A corepressors (Deheuninck and Luo, 2009).

Ski causes morphological transformation, *in vitro* and *in vivo*, of several avian cellular lineages (Colmenares et al., 1991; Larsen et al., 1992). Thus, it has been considered an oncoprotein. However, emerging evidence in mammalian cells and tumors suggest that Ski functions not only as an oncogene but also as a tumor suppressor protein in certain human cell types (Azuma et al., 2005; Le Scolan et al., 2008; Poser et al., 2005; Zhu et al., 2007). Studies in *Ski* knock-out mice have also identified Ski as a tumor suppressor protein (Shinagawa et al., 2001), however no clear mechanism for this activity of Ski has yet been established. This dual pro-oncogenic and anti-oncogenic activity has also been described for the Ski's family member SnoN. The pro-oncogenic activity of SnoN was dependent on the antagonism of the TGF-β /Smad pathway (Zhu et al., 2007) and it functioned as a tumor suppressor by inducing premature senescence (Pan et al., 2009).

Ski protein levels vary through the cell cycle, with the highest levels being found in mitosis (Macdonald et al., 2004; Marcelain and Hayman, 2005). During this stage, Ski was also phosphorylated by cdk1/cyclinB kinase and localized to the mitotic spindle and centrosomes (Marcelain and Hayman, 2005). These observations suggested the involvement of Ski in the mitotic process.

During mitosis, several mechanisms are activated to faithfully transmit genetic information to daughter cells. Specifically, the activation of the spindle assembly checkpoint (SAC) stops cell division until all chromosomes are attached to the mitotic spindle, and thus guarantees an even distribution of chromosomes to the daughter cells (reviewed in (Musacchio and Salmon, 2007) and (Bharadwaj and Yu, 2004)). Furthermore, if aberrant cells do divide, a special type of cell death called mitotic catastrophe is triggered (Castedo et al., 2004). Defects in these processes lead to aneuploidy, which is one of the most frequent manifestations of chromosomal instability in tumors and is closely associated with cancer progression and poor prognosis (Draviam et al., 2004; Rajagopalan and Lengauer, 2004).

In this paper we addressed the involvement of Ski in the mitotic process by analyzing mitosis and genomic stability in *Ski*−/− MEFs. We describe for the first time that *Ski*−/−MEFs exhibit high levels of aneuploidy resulting from defects in chromosome segregation and a weakened spindle assembly checkpoint. Furthermore, ectopic expression of Ski sensitised aneuploid cells to mitosis-associated cell death. These findings establish a new role for Ski in the mitotic process and in the mitotic aberration-induced cell death, providing insights into the mechanism of tumor suppression mediated by this protein.

## Materials and Methods

### Cell Culture and Transfection

Mouse embryo fibroblasts (MEFs) were isolated from *Ski*−/−, *Ski*+/− and wt embryos at 14.5 and 15.5 d.p.c. (Colmenares et al., 2002). WT SV-40 immortalized MEFs were kindly provided by Dr. Claudio Hetz (Programa de Biología Celular y Molecular, ICBM, U. de Chile). Early passage (p2–6) and immortalized (p>20) MEFs were maintained in Dulbecco's modified Eagle's medium(Invitrogen) supplemented with 10% fetalbovine serum (FBS), Glutamine, penicillin G (100 units/ml), and streptomycin(100 mg/ml).

### Plasmid Constructs and Retrovirus-mediated Gene Transfer

Rebna-H2B-GFP plasmid was provided by Dr. O. Petrenko, Stony Brook University. Tet-regulated hSki expressing MEFs were established as described previously (Zhao et al., 2009).

Phoenix E packaging cells were transfected (*Trans*IT-LT1, Mirus, Madison, USA) and grown for 48h toconfluence prior to harvesting the viral supernatant. MEFs were infected with the filtered supernatant supplemented with Polybrene (10μg/ml) and 10% FBS and then again after six hours. Theinfected cells were cultured for 48h and then selected for 3 days in the presence of hygromycin (100μg/ml) or puromycin (2μg/ml) for Tet-regulated Ski and H2B-GFP expressing cells, respectively.

### Indirect Immunofluorescence and microscopy

Cells were grown to exponential phase on poly-L-lysine-coated glass coverslips. Cell were fixed in paraformaldehyde, permeabilized in 0.1%TritonX-100 and blocked with image-IT Fix (Invitrogen). Primary antibodies used were: human anti-CREST serum (Antibodies Incorporated, 1:50 v/v), mouse anti-BubR1 and mouse anti-Bub3 (BD Bioscience, 1:100 v/v each). DNA was stained with Hoescht (Molecular Probes). Microscopy was performed using a DSU confocal microscope (Olympus, Inc.), using PlanApo-N60x/1.42 or PlansApo100x/1.4 oil objectives. Image editing was performed in Adobe Photoshop 6.0.

### Metaphase spreads

MEFs growing in exponential phase were incubated with 0.2 μg/ml colcemid (Calbiochem) for 4 h. Cells were harvested by trypsinization, swollen in 75 mM KCl at 37°C, fixed with 3:1 methanol/acetic acid (v/v), and dropped onto clean, ice-cold glass microscope slides. The slides were air-dried and stained with DAPI for 10 min. Chromosome numbers were evaluated using a Zeiss Axioskop microscope under a 100x/1.4 objective. At least 50 metaphases were analyzed per sample.

### Flow cytometry analysis

Exponentially growing cells were fixed in 80% ethanol and stained with 50 μg/ml propidiumiodide (PI) in the presence of 10 μg of DNase-free RNase per ml. For Histone H3 staining, fixed cells were pelleted and resuspended in 0.25% Triton X-100/0.1% BSA/PBS and left 15 minutes on ice. After washing, cells were incubated with rabbit anti-pS10H3 (Abcam, 1:300). Alexa-488 secondary antibody (Invitrogen) was used at 1:200. Cells were treated with RNase A and DNA stained with PI. Cell cycle profiles were determined by FACSDiVa (BD Bioscience) and data were analyzed using FCS Express V3 software. For the analysis of aneuploidy, Multicycle plug in was used.

### Protein extraction and immunoblotting

Whole cell extracts were prepared using CHIP lysis buffer (20mM Tris-HCl, pH 7.4, 140mM NaCl, 1% Triton X-100, 0.1% Sodium Deoxycholate, and protease and phosphatase inhibitor cocktails (Calbiochem)). For immunoblot detection the primary antibodies used were G8 anti-v-Ski, anti-cyclin B1 (Santa Cruz Biotechnology), anti-βActin (Sigma), anti-BubR1 (BD Bioscience), anti-Bub3 (BD Bioscience) and anti-αTubulin (Sigma).

### Time-Lapse Microscopy

H2B-GFP expressing MEFs were grown on poly-L-Lysine-coated glass bottom dishes (MatTek Corporation, USA) and synchronized by double thymidine block: 2mM Thymidine for 16h, Fresh medium for 10h, 2mM Thymidine for 15h. Block release was performed in DMEM 10% FBS without phenol red. Eight to 10 hours after release, cells were imaged with an Axioskop 2 microscope (Carl Zeiss, Inc.) fitted with a 63x/0.75LD Achroplan objective lens. Temperature, humidity and $CO_2$ were controlled in a stage-top incubator (Carl Zeiss, Inc.). Images were acquired every 3 to 5 minutes using Axiovision software (Carl Zeiss, Inc.). Six to 8 z-stacks were imaged at each time point. The phase contrast channel was imaged only at the beginning and at the end of the experiment, in order to avoid detrimental over exposure to light. Selected z-stacks and time points were used to compose figures and movies using ImageJ software.

## Results

### Aneuploidy in *Ski*−/− Mouse Embryonic Fibroblasts (MEFs)

In order to investigate the potential role of Ski during mitosis, we evaluated the ploidy status of proliferative embryonic fibroblasts (MEFs) isolated from *Ski* knockout (*Ski*−/−) mice (Colmenares et al., 2002). Chromosome counts from metaphase spreads showed that a majority of WT and Ski heterozygous (*Ski*+/−) cells had a 2n=40, while *Ski*−/− MEFs had a wide range and highly variable number of chromosomes, ranging from 33 to 75 chromosomes. Importantly, most cells had between 38 and 42 chromosomes, indicating the loss or gain of a few chromosomes (Figure 1a). A representative example of chromosome spreads from a *Ski* WT, *Ski*+/− and *Ski*−/− MEFs are shown in Figure 1b. Aneuploidy increased in spontaneously immortalized *Ski*−/− but not in *Ski*+/− MEFs (p.>30) or in SV40-immortalized WT MEFs. Representative chromosome spreads are shown in Figure 1c. Flow cytometry analysis of DNA content showed an average of about 68% aneuploidy in *Ski*−/− immortalized MEFs, while only about 10% and 8.5 % of *Ski*+/− and *Ski* WT immortalized cells were aneuploid, respectively (Figure 1d).

### Aberrant mitotic progression and defective chromosome segregation in Ski−/− cells

In order to help establish the mechanism leading to aneuploidy in the *Ski*−/− cells, we monitored the mitotic process *in vivo*. By retroviral transduction we generated cells that constitutively expressed a GFP-H2B fusion protein, which stays associated with chromosomal DNA throughout mitosis and thus allowed us to follow the progression of mitotic cells *in vivo*. Time-lapse studies revealed an important number of defects in the mitotic process of the *Ski*−/− cells. Most of these defects were present at Metaphase/Anaphase. Among cells that completed mitosis, 82% had at least one of the following aberrations: lagging chromosomes, chromosome bridges or chromatin bridges. Furthermore, approximately 50% of *Ski*−/− cells ended up with micronuclei (MN) (Figure 2a and b and Supplementary Videos S1 and S2). As control, we used *Ski*+/− MEFs since we considered these cells to constitute a more accurate control than WT MEFs since both *Ski*−/−and *Ski*+/− MEFs have an increased proliferation rate as compared to WT MEFs (Shinagawa et al., 2001), and could thus be handled in parallel. Furthermore, as seen in Figure 1, even after

multiple passages the *Ski*+/− cells were not significantly different than WT MEFs, having lower levels of aneuploidy than even early passage *Ski*−/− cells. We found that only 25% of heterozygous cells presented any of the aforementioned mitotic abnormalities. The other 75% of *Ski*+/− cells had no mitotic aberrations and the outcome of mitosis was two cells with interphase nuclei similar in size as predicted for a normal mitosis (Figure 2c). In a more detailed study, using fixed cells and immunofluorescence, we found that about 41% of *Ski*−/− MEFs exhibited micronuclei (MN) and 65% of *Ski*−/− cells exhibited chromatin and chromosome bridges and lagging chromosomes. These percentages were significantly higher than those in *Ski*+/− MEFs (Table 1). About 20% of the chromosomes involved in these aberrations were positive for one or two CREST signals, thus they were centromere-containing chromosomes (Figure 3). As all of these abnormalities are related to chromosome missegregation, these observations suggested that defective chromosome segregation could be responsible for the numerical chromosome aberrations displayed by the *Ski*−/− MEFs.

## The Spindle Assembly Checkpoint in *Ski* −/− cells

Chromosome segregation is controlled in part by the spindle assembly checkpoint (SAC). When chromosomes that have detached from microtubules are present in metaphase, the SAC is activated and this inhibits further mitotic progression and hence prevents abnormal chromosome segregation (Bharadwaj and Yu, 2004; Musacchio and Salmon, 2007). Whole chromosome loss during cell division, i.e. centromere containing chromosomes (Figure 3), suggested a defective SAC activation in the *Ski* −/− cells. As SAC activation involves a delay in the mitosis, we analyzed the total length of the mitotic process in the *Ski* −/− and the *Ski* +/− control cells. We considered this as the time-span from when chromosome condensation was first detected to the completion of cell division, as judged by cell flattening and DNA decondensation. We found that *Ski*−/− MEFs have a significantly longer mitosis than that of *Ski* +/− cells, with a mean of 87.1 minutes versus 56 minutes in the *Ski* +/− cells (Table 2 and Figure 2). This delay in the mitotic progress was a result of the significantly delayed Anaphase and maybe a prolonged Metaphase, although the difference in Metaphase was not clearly statistically different than *Ski*+/− cells (Table 2).

Importantly, among all *Ski*−/− cells analyzed (*N*=37), one third of the cells (*N*=12) were not included in the above analysis because they did not complete the mitotic process, at least during the recording time. These cells stayed at the Metaphase stage for >307 minutes. During this time, a dynamic metaphase plate re-arrangement was observed. Several conformations were adopted, changing the spatial distribution of the chromosomes from abnormally aligned to radial and back, in a clear attempt to reach a correct alignment of the chromosomes (Figure 4a and Supplementary Video S3). Remarkably, no *Ski*+/− cell was arrested in Metaphase, although a dynamic metaphase plate re-arrangement was also evident in some of these cells. But in contrast to the observations of *Ski*−/− cells, this chromosome reorganization in *Ski*+/− cells only took 38±3 minutes and after that time period, anaphase and the rest of the mitotic process took place normally (Figure 4b and Supplementary Video S4).

Therefore, it seems that SAC is active, but only in a subset of *Ski* −/− cells. We hypothesized that this activation is depending on the strength of the signaling; therefore we examined SAC activation using the maximal signal, i.e. by treating cells with microtubule depolymerizing drugs. We quantified the DNA content by flow cytometry and found that eight to twelve hours after colcemid treatment most *Ski*+/− and *Ski*−/− cells were evidently arrested at $G_2$/M, suggesting SAC activation (Figure 5a and b). Moreover, substantial cell death was evident twenty four hours after colcemid treatment, as indicated by an increased proportion of cells with sub-$G_1$ DNA content. Note that in *Ski*−/− cells, the accumulation in $G_2$/M was evident for cells with close to normal and higher than normal (polyploid) DNA content (Figure 5b). Changes in DNA content were accompanied by an increase in cyclin B1

protein levels in *Ski*+/− cells and in *Ski* −/− cells, as seen by western blotting (Figure 5c). SAC signaling involves inactivation of the Anaphase Promoting Complex (APC), which is responsible for degradation of key proteins during this phase of the cell cycle. As cyclin B is an APC target, the accumulation of cyclin B indicates that APC-dependent cyclin B proteosomal degradation is inhibited. However, the colcemid-induced increases of cyclin B levels were lower and less sustained in time in *Ski*−/− than in the *Ski*+/− cells.

To further analyze SAC activation, we evaluate the presence of two components of the SAC pathway, Bub3 and BubR1 proteins, in the *Ski*−/− and WT immortalized MEFs. We found that localization of these two proteins did not differ between *Ski*−/− and WT MEFs (Supplementary Figure 1). We found no differences in the total levels of Bub3, which remained stable after nocodazole treatment in WT and *Ski*−/− cells (Figure 6a). On the other hand, BubR1 levels increased upon treatment in WT and *Ski*−/− cells, however in WT cells, the increase was sustained up to 24 hours after treatment, whereas in *Ski*−/− at that point, the levels of BubR1 had decreased to levels comparable to untreated cells (time 0h). Studies of mitotic arrest by looking at DNA content are not completely straightforward in the *Ski*−/− cells given the high aneuploidy displayed by these cells. Thus, we measured the presence of histone H3 phosphorylated at serine 10 (a mitotic marker) in cells exposed to nocodazole for different times and found that H3pS10 increased after treatment, indicating accumulation of mitotic cells. But this increase was lower in *Ski*−/− than in WT cells (Figure 6b). These data altogether indicate that *Ski*−/− cells have an active but weakened SAC.

## Re-introduction of Ski leads to mitotic cell death

In order to assess whether re-expression of Ski could reverse the mitotic abnormalities observed in the *Ski*−/− cells, we introduced a *Ski* cDNA whose expression was driven by a Tet-regulated promoter in those cells. Thus, Ski expression could be induced by Doxycycline (tetracycline analog) withdrawal whereas addition of Doxycycline turned off Ski expression (Figure 7a). *In vivo* analysis of the mitotic process in the *Ski*−/− cells in which Ski expression was not induced (*Ski*−/−DOX+) revealed no differences with parental *Ski*−/− cells, i.e. two third of the cells completed mitosis. Whereas only 50% of *Ski*−/− cells expressing ectopic Ski (*Ski*−/−DOX−) completed mitosis during the recording time. In this population the time spent in mitosis (132±65.4 minutes, *N*=22) was significantly higher than for *Ski*+/− cells, but was not significantly different from the time in mitosis for *Ski*−/−DOX + cells (97±16 minutes). Among the Ski-expressing cells, about 67% had lagging chromosomes and/or chromatin bridges and the remaining 33% showed no apparent abnormality.

The remaining 50% of *Ski*−/−DOX− MEFs failed to complete mitosis. Analysis of this cohort of cells indicated that about 65% of these cells died after aberrant cell division and the remaining 35% showed Metaphase arrest similar to *Ski*−/− cells. During this time, chromosome reorganization was again observed. However, chromosome morphology was lost with signs of DNA decondensation and subsequently, DNA condensation and/or fragmentation. At this point those cells showed changes characteristic of cell death (Figure 7b–c and Supplementary Videos S5 and S6) and importantly none of these changes were observed in any of the *Ski*+/−, *Ski*−/− or *Ski*−/−DOX+ cells.

Time elapsed from the first chromosome alignment (Metaphase) to DNA decondensation and loss of chromosome morphology (signaling cell death) was 73±31 minutes in the *Ski*−/−DOX− cells (now expressing Ski). Although this time was dramatically shorter than the recorded time for *Ski*−/− cells arrested in Metaphase (>307 min), we could not rule out that in the absence of Ski these cells would also eventually die after a prolonged period of time. Thus, in order to have a quantitative estimation of Ski-induced mitotic cell death, we evaluated nuclear morphology and quantified cells showing evidence of apoptosis and/or

mitotic catastrophe in *Ski*−/− MEFs, with and without induction of Ski expression. Mitotic catastrophe has been described as an aberrant form of mitosis-associated cell death characterized by the occurrence of gigantic cells with several nuclei corresponding to individual clusters of missegregated chromosomes (Castedo et al., 2004; Vakifahmetoglu et al., 2008). An example of a cell with these characteristics is shown in Supplementary Figure 2. We found that only 1% of *Ski*−/− cells had nuclei with this death-associated morphology and this percentage increased approximately 10-fold upon induction of Ski expression in the *Ski*−/− cells (Table 3). It is important to notice that more than 80% of the cell death observed corresponded to mitotic catastrophe. This increase in cell death also correlated with a significant decrease in micronuclei-containing cells observed upon Ski expression (35% *v/s* 41.5%, $p<0,05$). Taken together these data indicate that ectopic expression of Ski in the *Ski*−/− cells leads to mitotic catastrophe primarily in cells with micronuclei, thus decreasing the number of aberrant cells that had been generated by defective chromosome segregation.

## Discussion

Aneuploidy, defined as an unbalanced number of chromosomes or large portions of chromosomes (Geigl et al., 2008), is the most frequent manifestation of genomic instability in human malignancies (Kops et al., 2005; Sen, 2000). Mechanisms that can give rise to aneuploid cells include amplification of centrosomes and defects in the mitotic process, including inappropriate attachment of chromosomes to the mitotic spindle or partial inactivation of the spindle checkpoint (SAC) (reviewed by (King, 2008)).

Previous studies showed that Ski protein levels increased during mitosis (Macdonald et al., 2004; Marcelain and Hayman, 2005). During this phase of the cell cycle, Ski is phosphorylated by cdk1, localizes to the mitotic spindle and is a *bona fide* component of the centrosomes (Marcelain and Hayman, 2005). These findings suggested a role for Ski during mitosis. In this work we show that the absence of Ski in MEFs generates a high level of genomic instability. This instability arises as a result of defective chromosome segregation, a weakened SAC and a failure of aberrant cells to undergo cell death. Genomic instability, manifested as aneuploidy in *Ski*−/− MEFs, was not the result of prolonged culture as it was evident in early as well as in late passages (Figure 1). In addition, *Ski*+/− MEFs, used as control, were manipulated in parallel to *Ski*−/− cells and thus had the same passage number at each experimental point. These control cells had significantly lower aneuploidy. Lagging chromosomes and chromatin bridges resulted in micronuclei formation and subsequent gain or loss of chromosomes in the *Ski*−/− cells. We assume that as a consequence of these defects, the *Ski*−/− cells spent a prolonged time in the metaphase and anaphase stages of mitosis, which resulted in an extension in the total mitotic process (Table 2).

From our *in vivo* analysis of mitotic cells, we identified two groups of *Ski*−/− cells. The first group is composed of cells with chromosomal alignment and segregation defects. These cells spent a longer time before anaphase than control cells, suggesting SAC activation. Nevertheless, a high percentage of these cells did complete mitosis but exhibited lagging chromosomes, indicating that SAC was insufficient to prevent chromosomal missegregation. Moreover, when we induced a “full” SAC, by using de-polymerizing drugs, *Ski*−/− cells did arrest at mitosis, but in a lesser extend than control cells. Thus, we conclude that these cells have a weakened SAC which is sufficient to stop cell division when signaling is coming from all kinetochores but insufficient to prevent missegregation of few unattached chromosomes. A weakened SAC has also been shown for cells with diminished levels of Aurora B (Hauf et al., 2003), CENP-I/Mis6 (Liu et al., 2003), CENP-E (Weaver et al., 2003) and Bub1 (Johnson et al., 2004) and it has been proposed to be responsible for chromosome instability and aneuploidy in tumors, as a weakened checkpoint signal is sufficient for

maintaining a viable population of cells that missegregate small numbers of chromosomes per division (Weaver and Cleveland, 2005).

The second group of *Ski*−/− cells showed a long metaphase arrest and did not progress to anaphase during the recorded time (up to 307 min). Particularly interesting was the dynamic metaphase plate rearrangements observed during this arrest, which appeared to involve dynamic spindle rearrangements since the metaphase plates switched polarity several times during recording (Figure 4). These dynamic rearrangements were also observed in a low percentage of control cells with lagging chromosomes. However, in these control cells the process took less time and the cells divided normally. This polarity switch of metaphase plates has been described for multipolar cells (Gisselsson et al., 2008). In our system, control cells were bipolar; therefore these polarity switches are not exclusive for multipolar mitoses. We speculate that the dynamic microtubule-chromosome associations are indicative of SAC activation or an attempt to "correct" the defective alignment. In this sense, SAC activation would not only involve stopping mitosis progression, but also be an active mechanism of chromosome alignment adjustment. Moreover, this chromosomal adjustment was associated with mitotic cell death. After ectopic expression of Ski, *Ski*−/−cells displaying the dynamic chromosome rearrangement failed to progress to anaphase. After several switches in polarity, those cells went from metaphase to cell death. This cell death was not observed either in control cells or in cells lacking Ski.

In the presence of strong checkpoint signaling (Figure 5), cells without Ski undergo cell death. But in the absence of a strong checkpoint signal, even after a prolonged mitotic arrest, cells lacking Ski are incapable of executing a cell death pathway. Thus it seems that Ski is not essential for inducing the death of aberrant mitotic cells when checkpoint signaling is activated through signals from all kinetochores, but it is needed to transduce a cell death signaling when only a few misaligned chromosomes are present. It has been propose that a prolonged metaphase arrest would result in the accumulation of pro-apoptotic complexes, which are currently unidentified (Weaver and Cleveland, 2005). Ski could be part of those complexes, providing a link between the SAC machinery and mitotic cell death.

Several studies have shown that HDAC activity is required for maintenance of pericentric heterochromatin, centromere function (Eot-Houllier et al., 2008; Taddei et al., 2001) and sister chromatid cohesion (Eot-Houllier et al., 2008; Kimata et al., 2008). Down-regulation or pharmacological inhibition of HDAC3 results in premature sister chromatid separation, defective chromosome condensation, misaligned and missegregated chromosomes; impaired mitotic progression in living cells with chromatin bridges and lagging chromosomes; significant lengthening or even a block at prometaphase and metaphase (Cimini et al., 2003) ; and cell death (Dowling et al., 2005). Furthermore a recent study reported the localization of an HDAC3 complex, including the nuclear receptor corepressor (N-CoR), to the mitotic spindle and showed that HDAC3 or N-CoR knockdown leads to chromosome misalignment, impaired kinetochore–microtubule attachment, and mitotic spindle collapse (Ishii et al., 2008). We have showed that Ski and HDAC3 are associated and Ski can inhibit proteasomal degradation of HDAC3, and consequently endogenous levels of HDAC3 are lower in the *Ski*−/− MEF than WT MEF (Zhao et al., 2009). Given the similarities displayed by *Ski*−/− MEF and cells in which HDAC activity was inhibited, it is possible that the mitotic defects identified in the absence of Ski could be related to Ski's ability to stabilize the HDAC3 co-repressor complexes. Further studies need to be conducted to determine the presence of Ski co-repressor complexes activity in mitotic chromosomes in order to provide a link between chromosome structure, SAC activation and mitotic cell death.

## Supplementary Material

Refer to Web version on PubMed Central for supplementary material.

## Acknowledgments

This work was supported by U.S. Public Health Service, National Cancer Institute Grants CA42573 (M.J.H.) and T32-CA009176 (NU); Vicerrectoría de Investigación y Desarrollo (VID) Grant I07/11-2 from Universidad de Chile (K.M) and Fondo de Financiamiento de Centros de Excelencia en Investigación (FONDAP) 15010006 (KM and RA).

## References

Akiyoshi S, Inoue H, Hanai J, Kusanagi K, Nemoto N, Miyazono K, Kawabata M. c-Ski acts as a transcriptional co-repressor in transforming growth factor-beta signaling through interaction with smads. J Biol Chem. 1999; 274(49):35269–35277. [PubMed: 10575014]

Azuma H, Ehata S, Miyazaki H, Watabe T, Maruyama O, Imamura T, Sakamoto T, Kiyama S, Kiyama Y, Ubai T, Inamoto T, Takahara S, Itoh Y, Otsuki Y, Katsuoka Y, Miyazono K, Horie S. Effect of Smad7 expression on metastasis of mouse mammary carcinoma JygMC(A) cells. J Natl Cancer Inst. 2005; 97(23):1734–1746. [PubMed: 16333029]

Bharadwaj R, Yu H. The spindle checkpoint, aneuploidy, and cancer. Oncogene. 2004; 23(11):2016–2027. [PubMed: 15021889]

Castedo M, Perfettini JL, Roumier T, Andreau K, Medema R, Kroemer G. Cell death by mitotic catastrophe: a molecular definition. Oncogene. 2004; 23(16):2825–2837. [PubMed: 15077146]

Cimini D, Mattiuzzo M, Torosantucci L, Degrassi F. Histone hyperacetylation in mitosis prevents sister chromatid separation and produces chromosome segregation defects. Mol Biol Cell. 2003; 14(9):3821–3833. [PubMed: 12972566]

Colmenares C, Heilstedt HA, Shaffer LG, Schwartz S, Berk M, Murray JC, Stavnezer E. Loss of the SKI proto-oncogene in individuals affected with 1p36 deletion syndrome is predicted by strain-dependent defects in Ski−/− mice. Nat Genet. 2002; 30(1):106–109. [PubMed: 11731796]

Colmenares C, Sutrave P, Hughes SH, Stavnezer E. Activation of the c-ski oncogene by overexpression. J Virol. 1991; 65(9):4929–4935. [PubMed: 1870207]

Chen D, Xu W, Bales E, Colmenares C, Conacci-Sorrell M, Ishii S, Stavnezer E, Campisi J, Fisher DE, Ben-Ze'ev A, Medrano EE. SKI activates Wnt/beta-catenin signaling in human melanoma. Cancer Res. 2003; 63(20):6626–6634. [PubMed: 14583455]

Dahl R, Kieslinger M, Beug H, Hayman MJ. Transformation of hematopoietic cells by the Ski oncoprotein involves repression of retinoic acid receptor signaling. Proc Natl Acad Sci U S A. 1998; 95(19):11187–11192. [PubMed: 9736711]

Deheuninck J, Luo K. Ski and SnoN, potent negative regulators of TGF-beta signaling. Cell Res. 2009; 19(1):47–57. [PubMed: 19114989]

Dowling M, Voong KR, Kim M, Keutmann MK, Harris E, Kao GD. Mitotic spindle checkpoint inactivation by trichostatin a defines a mechanism for increasing cancer cell killing by microtubule-disrupting agents. Cancer Biol Ther. 2005; 4(2):197–206. [PubMed: 15753652]

Draviam VM, Xie S, Sorger PK. Chromosome segregation and genomic stability. Curr Opin Genet Dev. 2004; 14(2):120–125. [PubMed: 15196457]

Eot-Houllier G, Fulcrand G, Watanabe Y, Magnaghi-Jaulin L, Jaulin C. Histone deacetylase 3 is required for centromeric H3K4 deacetylation and sister chromatid cohesion. Genes Dev. 2008; 22(19):2639–2644. [PubMed: 18832068]

Geigl JB, Obenauf AC, Schwarzbraun T, Speicher MR. Defining 'chromosomal instability'. Trends Genet. 2008; 24(2):64–69. [PubMed: 18192061]

Gisselsson D, Hakanson U, Stoller P, Marti D, Jin Y, Rosengren AH, Stewenius Y, Kahl F, Panagopoulos I. When the genome plays dice: circumvention of the spindle assembly checkpoint and near-random chromosome segregation in multipolar cancer cell mitoses. PLoS One. 2008; 3(4):e1871. [PubMed: 18392149]

Hauf S, Cole RW, LaTerra S, Zimmer C, Schnapp G, Walter R, Heckel A, van Meel J, Rieder CL, Peters JM. The small molecule Hesperadin reveals a role for Aurora B in correcting kinetochore-microtubule attachment and in maintaining the spindle assembly checkpoint. J Cell Biol. 2003; 161(2):281–294. [PubMed: 12707311]

Ishii S, Kurasawa Y, Wong J, Yu-Lee LY. Histone deacetylase 3 localizes to the mitotic spindle and is required for kinetochore-microtubule attachment. Proc Natl Acad Sci U S A. 2008; 105(11):4179–4184. [PubMed: 18326024]

Johnson VL, Scott MI, Holt SV, Hussein D, Taylor SS. Bub1 is required for kinetochore localization of BubR1, Cenp-E, Cenp-F and Mad2, and chromosome congression. J Cell Sci. 2004; 117(Pt 8): 1577–1589. [PubMed: 15020684]

Kimata Y, Matsuyama A, Nagao K, Furuya K, Obuse C, Yoshida M, Yanagida M. Diminishing HDACs by drugs or mutations promotes normal or abnormal sister chromatid separation by affecting APC/C and adherin. J Cell Sci. 2008; 121(Pt 7):1107–1118. [PubMed: 18354085]

King RW. When 2+2=5: the origins and fates of aneuploid and tetraploid cells. Biochim Biophys Acta. 2008; 1786(1):4–14. [PubMed: 18703117]

Kops GJ, Weaver BA, Cleveland DW. On the road to cancer: aneuploidy and the mitotic checkpoint. Nat Rev Cancer. 2005; 5(10):773–785. [PubMed: 16195750]

Larsen J, Beug H, Hayman MJ. The v-ski oncogene cooperates with the v-sea oncogene in erythroid transformation by blocking erythroid differentiation. Oncogene. 1992; 7(10):1903–1911. [PubMed: 1408132]

Le Scolan E, Zhu Q, Wang L, Bandyopadhyay A, Javelaud D, Mauviel A, Sun L, Luo K. Transforming growth factor-beta suppresses the ability of Ski to inhibit tumor metastasis by inducing its degradation. Cancer Res. 2008; 68(9):3277–3285. [PubMed: 18451154]

Li Y, Turck CM, Teumer JK, Stavnezer E. Unique sequence, ski, in Sloan-Kettering avian retroviruses with properties of a new cell-derived oncogene. J Virol. 1986; 57(3):1065–1072. [PubMed: 3754014]

Liu ST, Hittle JC, Jablonski SA, Campbell MS, Yoda K, Yen TJ. Human CENP-I specifies localization of CENP-F, MAD1 and MAD2 to kinetochores and is essential for mitosis. Nat Cell Biol. 2003; 5(4):341–345. [PubMed: 12640463]

Luo K, Stroschein SL, Wang W, Chen D, Martens E, Zhou S, Zhou Q. The Ski oncoprotein interacts with the Smad proteins to repress TGFbeta signaling. Genes Dev. 1999; 13(17):2196–2206. [PubMed: 10485843]

Macdonald M, Wan Y, Wang W, Roberts E, Cheung TH, Erickson R, Knuesel MT, Liu X. Control of cell cycle-dependent degradation of c-Ski proto-oncoprotein by Cdc34. Oncogene. 2004; 23(33): 5643–5653. [PubMed: 15122324]

Marcelain K, Hayman MJ. The Ski oncoprotein is upregulated and localized at the centrosomes and mitotic spindle during mitosis. Oncogene. 2005; 24(27):4321–4329. [PubMed: 15806149]

Musacchio A, Salmon ED. The spindle-assembly checkpoint in space and time. Nat Rev Mol Cell Biol. 2007; 8(5):379–393. [PubMed: 17426725]

Nomura T, Khan MM, Kaul SC, Dong HD, Wadhwa R, Colmenares C, Kohno I, Ishii S. Ski is a component of the histone deacetylase complex required for transcriptional repression by Mad and thyroid hormone receptor. Genes Dev. 1999; 13(4):412–423. [PubMed: 10049357]

Pan D, Zhu Q, Luo K. SnoN functions as a tumour suppressor by inducing premature senescence. Embo J. 2009; 28(22):3500–3513. [PubMed: 19745809]

Poser I, Rothhammer T, Dooley S, Weiskirchen R, Bosserhoff AK. Characterization of Sno expression in malignant melanoma. Int J Oncol. 2005; 26(5):1411–1417. [PubMed: 15809735]

Rajagopalan H, Lengauer C. Aneuploidy and cancer. Nature. 2004; 432(7015):338–341. [PubMed: 15549096]

Sen S. Aneuploidy and cancer. Curr Opin Oncol. 2000; 12(1):82–88. [PubMed: 10687734]

Shinagawa T, Nomura T, Colmenares C, Ohira M, Nakagawara A, Ishii S. Increased susceptibility to tumorigenesis of ski-deficient heterozygous mice. Oncogene. 2001; 20(56):8100–8108. [PubMed: 11781823]

Stavnezer E, Barkas AE, Brennan LA, Brodeur D, Li Y. Transforming Sloan-Kettering viruses generated from the cloned v-ski oncogene by in vitro and in vivo recombinations. J Virol. 1986; 57(3):1073–1083. [PubMed: 3005612]

Sun Y, Liu X, Eaton EN, Lane WS, Lodish HF, Weinberg RA. Interaction of the Ski oncoprotein with Smad3 regulates TGF-beta signaling. Mol Cell. 1999; 4(4):499–509. [PubMed: 10549282]

Tabata T, Kokura K, Ten Dijke P, Ishii S. Ski co-repressor complexes maintain the basal repressed state of the TGF-beta target gene, SMAD7, via HDAC3 and PRMT5. Genes Cells. 2009; 14(1): 17–28. [PubMed: 19032343]

Taddei A, Maison C, Roche D, Almouzni G. Reversible disruption of pericentric heterochromatin and centromere function by inhibiting deacetylases. Nat Cell Biol. 2001; 3(2):114–120. [PubMed: 11175742]

Ueki N, Zhang L, Hayman MJ. Ski can negatively regulates macrophage differentiation through its interaction with PU.1. Oncogene. 2008; 27(3):300–307. [PubMed: 17621263]

Vakifahmetoglu H, Olsson M, Zhivotovsky B. Death through a tragedy: mitotic catastrophe. Cell Death Differ. 2008; 15(7):1153–1162. [PubMed: 18404154]

Weaver BA, Bonday ZQ, Putkey FR, Kops GJ, Silk AD, Cleveland DW. Centromere-associated protein-E is essential for the mammalian mitotic checkpoint to prevent aneuploidy due to single chromosome loss. J Cell Biol. 2003; 162(4):551–563. [PubMed: 12925705]

Weaver BA, Cleveland DW. Decoding the links between mitosis, cancer, and chemotherapy: The mitotic checkpoint, adaptation, and cell death. Cancer Cell. 2005; 8(1):7–12. [PubMed: 16023594]

Xu W, Angelis K, Danielpour D, Haddad MM, Bischof O, Campisi J, Stavnezer E, Medrano EE. Ski acts as a co-repressor with Smad2 and Smad3 to regulate the response to type beta transforming growth factor. Proc Natl Acad Sci U S A. 2000; 97(11):5924–5929. [PubMed: 10811875]

Zhang H, Stavnezer E. Ski regulates muscle terminal differentiation by transcriptional activation of Myog in a complex with Six1 and Eya3. J Biol Chem. 2009; 284(5):2867–2879. [PubMed: 19008232]

Zhao HL, Ueki N, Marcelain K, Hayman MJ. The Ski protein can inhibit ligand induced RARalpha and HDAC3 degradation in the retinoic acid signaling pathway. Biochem Biophys Res Commun. 2009; 383(1):119–124. [PubMed: 19341714]

Zhu Q, Krakowski AR, Dunham EE, Wang L, Bandyopadhyay A, Berdeaux R, Martin GS, Sun L, Luo K. Dual role of SnoN in mammalian tumorigenesis. Mol Cell Biol. 2007; 27(1):324–339. [PubMed: 17074815]

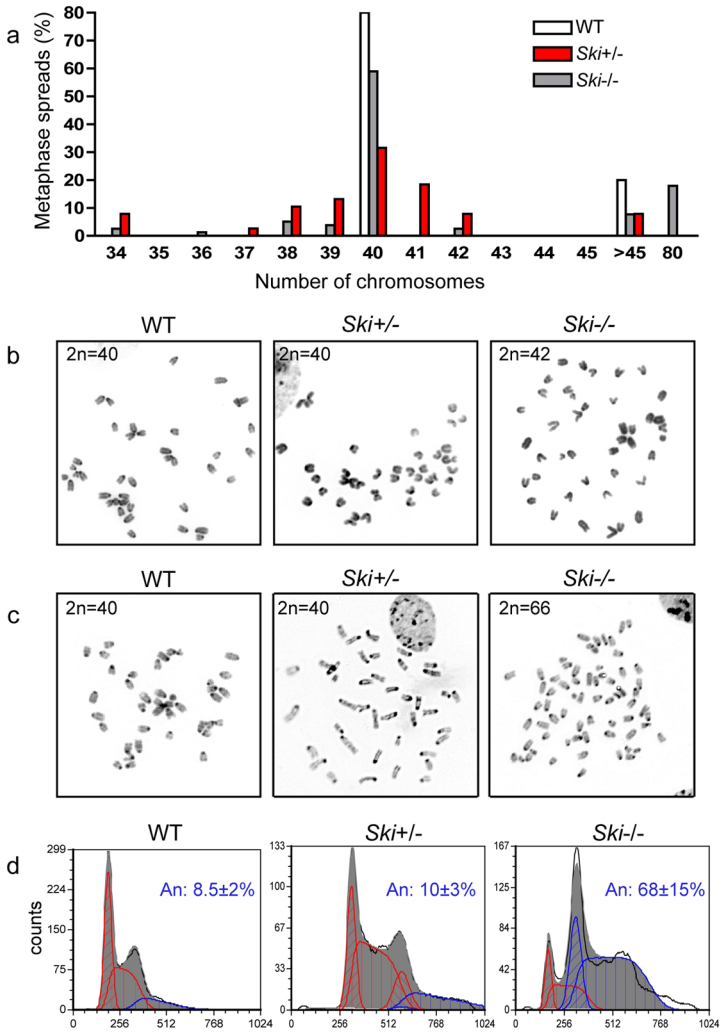


**Figure 1. Aneuploidy in *Ski*−/− Mouse Embryonic Fibroblasts (MEFs)**

**(a)** Determination of chromosomes number was done in metaphase spreads from early passage (p.<6) wild type (WT), *Ski*+/− and *Ski*−/− MEFs. **(b)** Representative metaphase spreads from early passage MEFs are shown. **(c)** Representative metaphase spreads from immortalized WT, *Ski*+/− and *Ski*−/− MEFs. **(d)** DNA content histograms of WT, *Ski*+/− and *Ski*−/− immortalized MEFs. Diploid (red) and aneuploid (blue) populations can be distinguished. The average aneuploidy percentage of cells from 2 different animals of each genotype is shown.

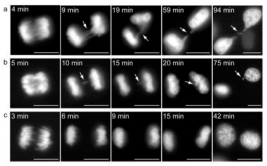


**Figure 2. Chromosome segregation defects in *Ski*−/− MEFs**

Mitotic *Ski*−/− and *Ski*+/−MEFs stably expressing a GFP-H2B fusion protein were analysed *in vivo* by time-lapse microscopy. Several z-stacks were acquired every five minutes. The most informative "t" and "z" frames were selected. **(a)** Chromatin bridges (arrows) in a *Ski* −/− cell leading to loss of genetic material. **(b)** Lagging chromosome (arrows) in a *Ski*−/− cell leading to micronucleus formation. **(c)** Normal chromosome segregation in a *Ski*+/− cell. Time, in minutes (min.), indicates time since anaphase starting. Scale bars: 10 μm. Movies showing the complete process are available as Supplementary videos (S1 and S2).

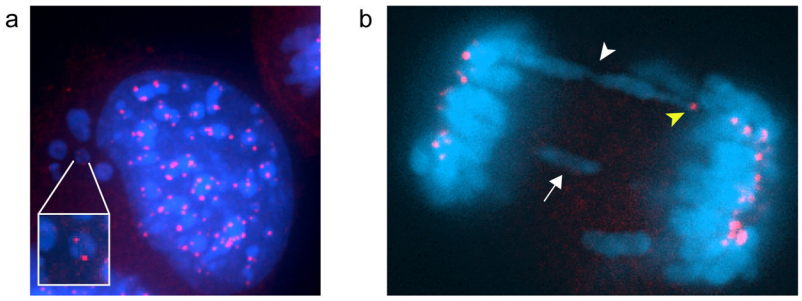


**Figure 3. Micronuclei and chromatin bridges in *Ski*−/− MEFs**

Centromeres (in red) were immunostained with an anti-CREST antibody and DNA with Hoescht (in blue). **(a)** Example of a cell containing several micronuclei. A magnified image of a micronucleus with two CREST signals is shown in the inset. The remaining micronuclei have one or none CREST signal. **(b)** A dividing cell with a lagging chromosome (arrow) and a chromosome bridge (white arrow head). One of the chromosomes involved in the bridge has a CREST signal (yellow arrow head).

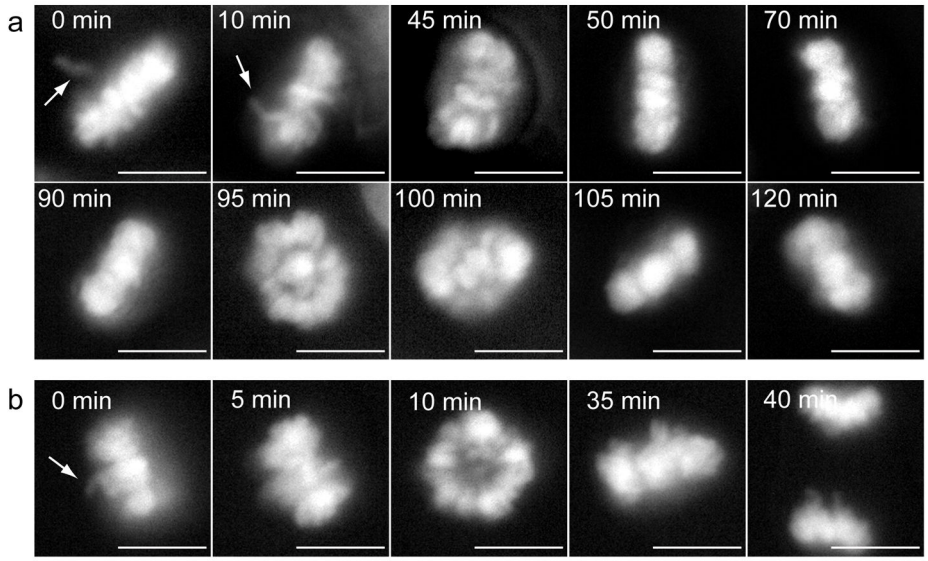


**Figure 4. Dynamic metaphase plate re-arrangement in *Ski*−/− MEFs arrested in metaphase and in *Ski*+/− cells**

Mitotic *Ski*−/− and *Ski*+/−MEFs were analysed as described in Figure 2. **(a)** *Ski*−/− cell arrested in metaphase for more than 120 minutes. Chromosomes remain aligned for 90 min, then a radial metaphase plate is evident and after 10 minutes, an apparently correct metaphase alignment is evident again. **(b)** A *Ski*+/− cell showing the same metaphase plate re-organization as in (a), but with different timing and outcome. Time, in minutes (min.), indicates time since first chromosome alignment. Arrows point to misaligned chromosomes. Scale bars: 10 μm. Movies showing the complete process are available as Supplementary videos (S3 and S4).

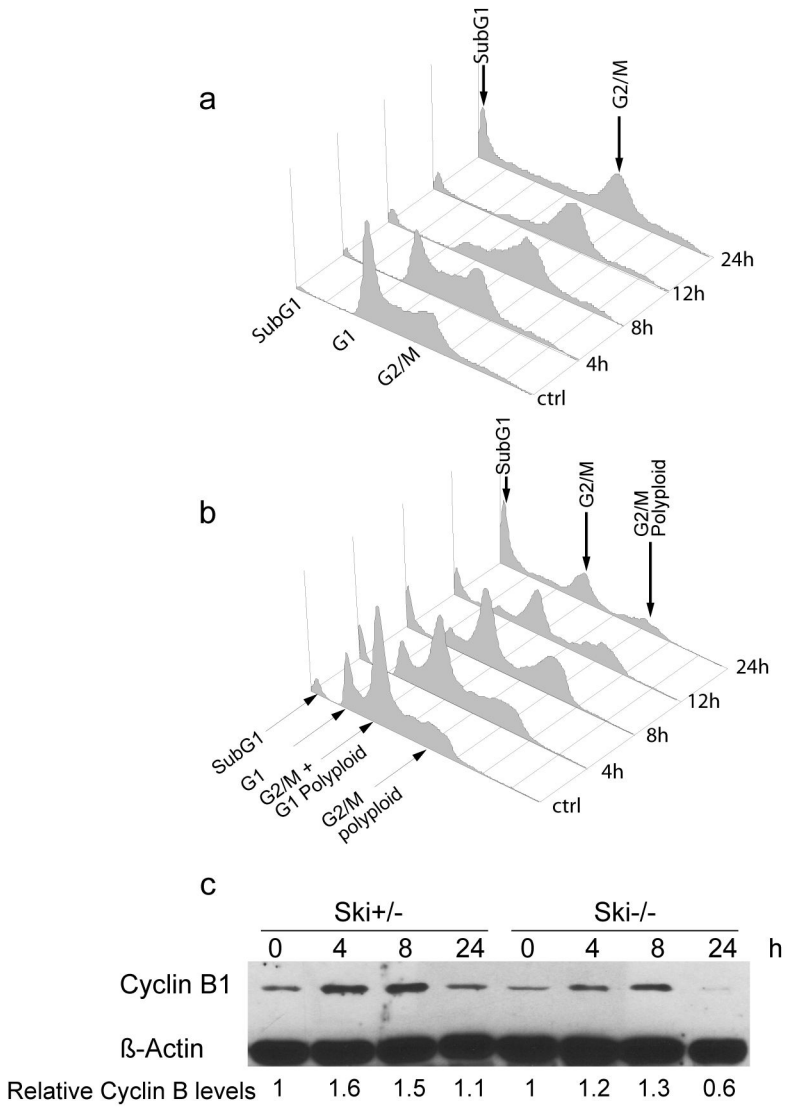


**Figure 5. Spindle Checkpoint activation in *Ski*+/− and *Ski*−/− MEFs**

DNA content histogram of *Ski*+/− **(a)** and *Ski*−/− **(b)** MEFs treated with colcemide (0,2 μg/ml) for 0 to 24 hours. **(c)** Cyclin B1 levels in *Ski*+/− and *Ski*−/− MEFs treated as in (a) determined by western blotting. β-Actin was used as loading control. Cyclin B bands were quantified, normalized to β-Actin and expressed as relative to time 0h (untreated cells). A representative experiment of at least three independent experiments is shown.

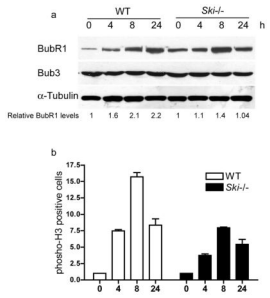


**Figure 6. Spindle Checkpoint activation in WT and *Ski*−/− MEFs**

WT and *Ski*−/− MEFs were treated with nocodazole (125ng/ml) for 0 to 24 hours. Levels of BubR1 and Bub3 were assessed by western blotting (a). BubR1 levels are expressed as relative to time 0h (untreated cells). A representative experiment is shown. (b) Cells positive for phosho-H3(S10) were determined by flow cytometry. Values are expressed as fold increase relative to time 0h (untreated cells).

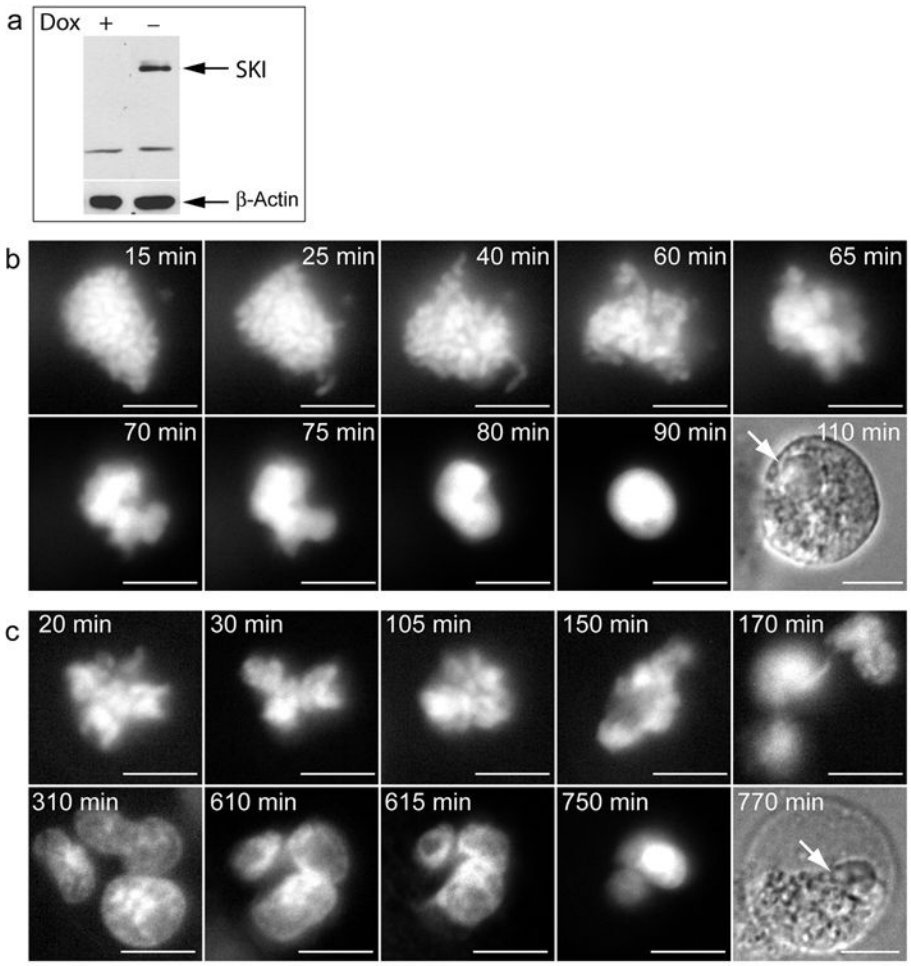


**Figure 7. Ski ectopic expression led to mitotic-associated cell death in *Ski*−/− MEFs**

**(a)** *Ski*−/− MEFs expressing Ski under the control of a doxycycline-regulated promoter were transduced to express a GFP-H2B fusion protein. 48 hours after Doxycycline withdrawal, Ski levels were monitored by western blotting in cells exposed or not to Doxycycline (Dox + and Dox −), using anti-Ski antibody. β-actin was used as loading control **(b and c)** Mitotic ski-expressing cells were analysed as described in Figure 2. Examples of cell death following sustained (Pro)Metaphase arrest and aberrant cell division are shown in **(b)** and **(c)**, respectively. Time, in minutes (min.), indicates time since nuclear envelop breakage. Arrows in bright field pictures indicate position of nuclei. Scale bars: 10 μm. Movies showing the complete cell death process are available as Supplementary videos (S5 and S6).

**Table 1**

Percentage of *Ski*+/− and *Ski*−/− MEF containing Micronuclei and Other Chromosome segregation abnormalities

| MEF Genotype[a] | % of cells with Micronuclei | % of cells with Other Segregation Defects[b] |
|---|---|---|
| *Ski*+/− | 30±6 | 13±1 |
| *Ski*−/− | 41.5±8* | 65±3* |

[a] Five-hundred cells of each cell type were examined. *N*=3 for each genotype

[b] Include Chromosome/chromatin bridges and lagging chromosomes

* $p<0.005$ compared to Ski+/− MEF (*Chi-Square* Test).

**Table 2**

Duration of mitosis in *Ski*+/− and *Ski*−/− MEF[a]

| MEF Genotype[b] | Total Length[c] | Metaphase | Anaphase | Telophase |
|---|---|---|---|---|
| *Ski*+/− | 56±4.8 | 27.2±7.9 | 3.8±0.4 | 37.1±0.9 |
| *Ski*−/− | 87.1±10.5* | 49.6±10.8 | 7.9±0.9* | 48.1±10.8 |

[a] Mean ±SE (in minutes) are shown.

[b] Twenty four cells of each cell type were examined.

[c] Time lapse since chromosome condensation was detected up to DNA decondensation after cell division. Only cells that completed mitosis were included in the analysis.

* $p<0.05$ compared to *Ski*+/− MEF (Unpaired *t* Test).

## Table 3

Quantification of Cell Death in Ski expressing (Dox−) and not expressing (Dox+) MEF

| Ski Expression[a] | Total no. of cell counted | No. of cells with cell death characteristics[b] | % of cells with cell death characteristics |
|---|---|---|---|
| *NO* | 348 | 4 | 1.1 |
| *YES* | 409 | 48 | 10.5* |

Abbreviation: Dox, Doxycycline

[a] Ski expression was induced by Doxycycline withdraw in Ski−/− MEF.

[b] Gigantic cells with fragmented non-condensed nuclei (Mitotic catastrophe, as shown in Supplementary Figure 1) and cells with highly condensed and/or fragmented DNA (Apoptosis, as in Figure 6).

* $p<0.001$ compared to Ski−/− MEF not expressing Ski (*Fisher's exact* Test).